The New LED-Sensitive Photoinitiators of Polymerization: Copper Complexes in Free Radical Photoinitiating Systems and 3D Printing

Timur Borjigin, Guillaume Noirbent, Didier Gigmes, Pu Xiao, Frédéric Dumur, Jacques Lalevée, Jacques Lalevée

The New LED-Sensitive Photoinitiators of Polymerization: Copper Complexes in Free Radical Photoinitiating Systems and 3D Printing

Timur Borjigin [1,2], Guillaume Noirbent[3], Didier Gigmes[3], Pu Xiao[4,*], Frédéric Dumur[3,*], Jacques Lalevée[1,2,*]

[1] Université de Haute-Alsace, CNRS, IS2M UMR 7361, F-68100 Mulhouse, France; timur1996x@hotmail.com(T.B)
[2] Université de Strasbourg, France
[3] Aix Marseille Univ, CNRS, ICR UMR 7273, F-13397 Marseille, France
[4] Research School of Chemistry, Australian National University, Canberra, ACT 2601, Australia
* Correspondence: pu.xiao@anu.edu.au (P.X.); frederic.dumur@univ-amu.fr (F.D.); jacques.lalevee@uha.fr (J.L.)

Abstract: A ligand (**A1**) and four copper complexes (**Cu1**, **Cu2**, **Cu3** and **Cu4**) were examined as photosensitizers in various photoinitiating systems (PISs). Interestingly, excellent photochemical reactivities were determined with the different compounds. Especially, notable photoinitiation abilities were determined upon exposure to LED@405 nm during the free radical polymerization of acrylates and the cationic polymerization of epoxides when combined with an iodonium salt and an amine. With regards to their remarkable reactivities, the different photoinitiating systems were applied to 3D printing experiments. By combining steady state photolysis and electron spin resonance spin trapping, the chemical mechanism supporting the polymerization processes could be fully detailed and proved. Among all PISs studied, the three-component PISs furnished the best monomer conversions during the free radical polymerization of trimethylolpropane triacrylate (TMPTA) and the cationic polymerization of (3,4-epoxycyclohexane)methyl 3,4-epoxycyclohexylcarboxylate (EPOX) monomers. The conversion process was monitored by real-time Fourier transform infrared spectroscopy (RT-FTIR). Three-component PISs based on **A1**, **Cu1** and **Cu2** showed better performances than those based on **Cu3**, **Cu4** and the different two-component PIS (comprising only the iodonium salt or the amine) in FRP experiments. Based on the outstanding photoinitiation abilities of **A1** and **Cu1** with both TMPTA and EPOX, smooth and regular 3D patterns could be obtained by direct laser write experiments by generating interpenetrating polymer networks (IPN) with the blend of these two monomers.

Keywords: copper complex; photoinitiator; free radical photopolymerization; IPN photopolymerization; photochemistry; LEDs; Direct laser writing; 3D printing

1. Introduction

As a key component of the photopolymerization process, photoinitiators are a class of compounds capable of generating reactive species (free radicals, cations, or anions) to initiate the polymerization reaction under light irradiation.[1-6] In recent years, with the development of new photocuring technologies, environmentally friendly and energy-saving light sources such as LEDs capable of emitting light in the visible range, photopolymerization is facing a revolution.[7] Parallel to this, sunlight has emerged as a cheap light source so that new challenges and scope of applications have emerged compared to that proposed by the traditional photoinitiators.[8-11] The development of photoinitiators absorbing in the visible range and exhibiting a high photosensitivity are actively researched.[12-16] Due to the presence of d orbitals, transition metals possess numerous molecular orbitals and the ligands used to create metal complexes can drastically impact both the position of the absorption maxima but also the molar extinction coefficient of the resulting metal complexes.[17-21] Parallel to this, the excited state lifetime can also be efficiently tuned. As other specificities, organometallic complexes often exhibit strong absorption bands resulting from metal/ligand interactions. Numerous transitions located in the near UV-Visible range are also often detected, resulting from π-π transitions centered on the organic ligands.[22-26] Indeed, an efficient strategy to complex a metal cation consists in using electron-rich polyaromatic structures, efficiently stabilizing the electron deficient metal cation.[27,28] Parallel to this, a careful selection of the organic ligands enables to efficiently control the light absorption properties of the complex (molar extinction coefficient, absorption maximum).[29,30] Chemical structures of these ligands can be

easily modified by molecular engineering. It thus brings a broad prospect for the diversity of photopolymerization reactions.

Due to their excellent electron donating abilities, transition metal complexes are candidates of choice for initiating photochemically induced electron transfer reactions and this ability has attracted a great deal of interest in various research fields.[30-33] Notably, transition metal complexes found numerous applications in organic synthesis, by mean of a process known as photoredox catalysis.[22] Metal complexes based on ruthenium[15,34] or iridium[35-40] are characterized by strong visible light absorption properties, long-living excited states and redox potentials adapted to efficiently react with the different additives (e.g., iodonium salts, amine, etc.) introduced into the photocurable resins. Notably, these complexes can be used to catalyze polymerization reactions by mean of oxidative or reductive catalytic cycles.[35,41,42] However, if highly performant, iridium and ruthenium complexes are facing numerous problems such as the limited availability of these two metals on Earth but also their costs and toxicity issues. Previous researches have established that copper complexes[12,43-46] could constitute a good alternative to iridium and ruthenium complexes due to their none or low toxicities, their low-costs, the easy availability of copper on Earth and their long-living excited state lifetimes. Xiao et al. [45] have reported a series of copper complexes developed as photocatalysts for free radical photopolymerization. Especially, the "G1" complex exhibited a good photoactivity, a high photoinitiation ability even at low photoinitiator content and under mild irradiation conditions. As a result of this, numerous copper complexes exhibiting different ligands have been synthesized and examined in various photoinitiating systems. Compared to other noble metal complexes used in photoredox catalysis, research on copper complexes is still far behind.

In this work, four copper complexes that have never been reported before have been designed and synthesized. In combination with an iodonium salt and a tertiary amine (ethyl dimethylaminobenzoate (EDB)), these copper complexes proved to be excellent candidates for initiating both free radical photopolymerizations (FRP) and cationic photopolymerizations (CP) of benchmark monomers i.e., TMPTA and EPOX respectively. By monitoring the polymerization process using Real-time Fourier Transform Infrared spectroscopy (RT-FTIR), the polymerization reactions could be carefully examined, and the conversion rate determined. Photochemical properties and mechanism of polymerization induced by the new photoinitiating systems were studied by steady state photolysis technique. In light of their remarkable reactivities in three-component systems, resins comprising the different complexes could be used in 3D printing experiments using TMPTA as the monomer. 3D Patterns based on interpenetrating polymer networks (IPN) that exhibited an excellent spatial resolution could also be obtained by direct laser write (DLW).

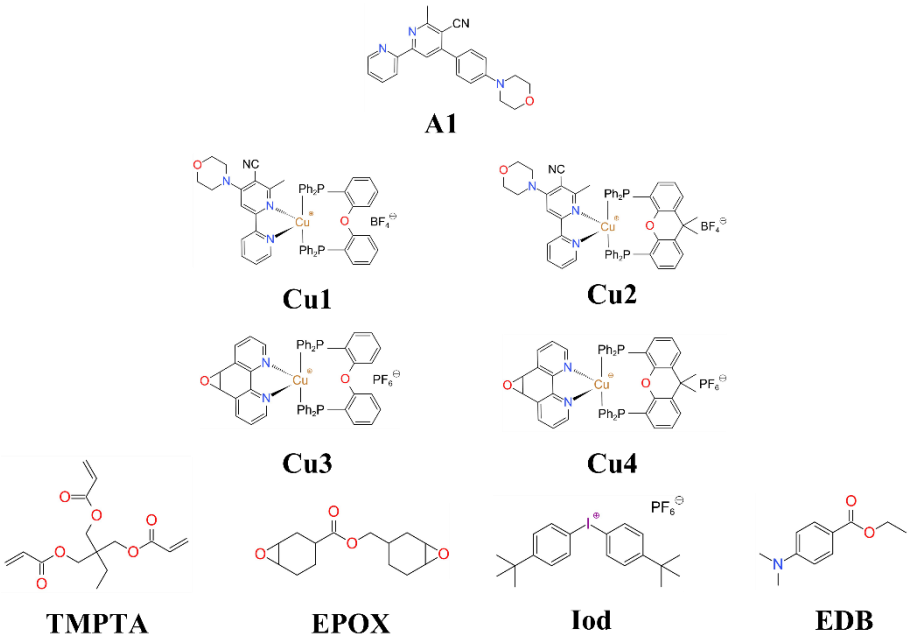

Scheme 1. Chemical structures of the studied ligand, copper complexes, iodonium salt (Iod), amine (EDB) and the monomers (TMPTA and EPOX)

2. Results and Discussion

2.1. Synthesis of the ligand and copper complexes

2.1.1. Synthesis of **A1**

A suspension of potassium *tert*-butoxide (1.2 g) in acetonitrile (300 mL) and β-aminocrotonitrile (4.92 g, 60 mmol, M = 82.10 g/mol) was heated at 35°C for 15 minutes. Chalcone (*E*)-3-(4-morpholinophenyl)-1-(pyridin-2-yl)prop-2-en-1-one (2.94 g, 10.0 mmol, M = 294.35 g/mol) was added to the suspension and the resulting solution was stirred at room temperature for three days. After that, the mixture was filtered and washed with ethanol and water. The resulting yellow solid was dissolved in dichloromethane and the solution was filtered on a plug of SiO_2 using dichloromethane as the eluent. The solvent was removed under reduced pressure (2.74 g, 77% yield).

^{1}H NMR (400 MHz, $CDCl_3$) δ 8.69 (ddd, J = 4.7, 1.6, 0.8 Hz, 1H), 8.50 (d, J = 8.0 Hz, 1H), 8.40 (s, 1H), 7.85 (td, J = 7.8, 1.8 Hz, 1H), 7.71 – 7.64 (m, 2H), 7.35 (ddd, J = 7.5, 4.8, 1.1 Hz, 1H), 7.05 – 6.98 (m, 2H), 3.93 – 3.84 (m, 4H), 3.31 – 3.24 (m, 4H), 2.90 (s, 3H).

^{13}C NMR (75 MHz, $CDCl_3$) δ 162.60, 157.53, 154.97, 153.82, 152.37, 149.54, 137.18, 129.90, 127.09, 124.73, 122.26, 118.02, 115.05, 106.62, 66.88, 48.43, 24.52.

HRMS (ESI MS) m/z: theor: 356.1637 found: 356.1639 ($M^{+\cdot}$ detected).

2.1.2. Synthesis of **Cu1**

A mixture of tetrakis(acetonitrile)copper(I) tetrafluoroborate (314 mg, 1.0 mmol, M = 314.56 g/mol) and 4,5-*bis*(diphenylphosphino)-9,9-dimethylxanthene (578 mg, 1.0 mmol, M = 578.62 g/mol) in 100 mL of dichloromethane was stirred at 25 °C for 2 h and then treated with a solution 6-methyl-4-(4-morpholinophenyl)-[2,2'-bipyridine]-5-carbonitrile (356 mg, 1.0 mmol, M = 356.43 g/mol) in 50 mL of dichloromethane. The reaction mixture was stirred for an additional 1 h and filtered and the clear yellow filtrate concentrated to 5 mL. Diethyl ether was added into the resulting solution afforded yellow crystals of the complex (1023 mg, 94% yield).

^{1}H NMR (400 MHz, $CDCl_3$) δ 8.76 (d, J = 8.2 Hz, 1H), 8.44 (s, 1H), 8.15 (t, J = 7.9 Hz, 1H), 8.11 (d, J = 4.9 Hz, 1H), 7.86 (d, J = 9.0 Hz, 2H), 7.65 (dd, J = 7.8, 1.3 Hz, 2H), 7.34 (dd, J = 7.2, 5.6 Hz, 1H), 7.30 (t, J = 7.4 Hz, 4H), 7.17 (m, 6H), 7.12 (t, J = 7.7 Hz, 4H), 7.07 (d, J = 9.0 Hz, 2H), 7.05 – 6.96 (m, 4H), 6.92 – 6.84 (m, 4H), 6.69 – 6.62 (m, 2H), 3.90 – 3.83 (m, 4H), 3.36 – 3.30 (m, 4H), 2.25 (s, 3H), 1.81 (s, 3H), 1.71 (s, 3H).

^{13}C NMR (101 MHz, $CDCl_3$) δ 161.87, 155.00, 154.94, 154.91, 154.88, 153.20, 152.94, 151.04, 148.47, 140.03, 133.93, 133.15, 133.07, 132.99, 132.59, 132.51, 132.44, 131.57, 131.40, 131.33, 131.23, 131.15, 130.97, 130.47, 130.24, 129.17, 129.12, 129.09, 129.05, 127.43, 127.11, 125.53, 125.42, 120.48, 120.34, 120.20, 115.04, 107.80, 66.72, 65.92, 47.95, 36.24, 29.57, 27.00, 25.98, 15.36.

HRMS (ESI MS) m/z: theor: 997.2856 found: 997.2852 ($M^{+\cdot}$ detected).

2.1.3. Synthesis of **Cu2**

A mixture of tetrakis(acetonitrile)copper(I) tetrafluoroborate (314 mg, 1.0 mmol, M = 314.56 g/mol) and *bis*[2-(diphenylphosphino)phenyl]ether (538 mg, 1.0 mmol, M = 538.57 g/mol) in 100 mL of dichloromethane was stirred at 25 °C for 2 h and then treated with a solution 6-methyl-4-(4-morpholinophenyl)-[2,2'-bipyridine]-5-carbonitrile (356 mg, 1.0 mmol, M = 356.43 g/mol) in 50 mL of dichloromethane. This reaction mixture was stirred for an additional 1 h and filtered and the clear yellow filtrate concentrated to 5 mL. Diethyl ether was added into the resulting solution afforded yellow crystals of the complex (992 mg, 95% yield).

^{1}H NMR (400 MHz, $CDCl_3$) δ 8.70 (d, J = 8.2 Hz, 1H), 8.42 (s, 1H), 8.35 (d, J = 4.7 Hz, 1H), 8.14 (t, J = 7.4 Hz, 1H), 7.85 (d, J = 8.9 Hz, 2H), 7.38 (t, J = 7.4 Hz, 2H), 7.35 – 7.27 (m, 5H), 7.23 (m, 8H), 7.12 – 7.04 (m, 8H), 7.04 – 6.96 (m, 6H), 6.93 (m, 2H), 3.93 – 3.80 (m, 4H), 3.38 – 3.21 (m, 4H), 2.55 (s, 3H).

^{13}C NMR (101 MHz, $CDCl_3$) δ 162.43, 158.08, 158.02, 157.96, 154.69, 153.62, 151.17, 149.06, 139.84, 134.35, 133.08, 133.00, 132.92, 132.33, 131.37, 130.96, 130.79, 130.70, 130.63, 130.49, 130.36, 130.20, 129.13, 129.08, 128.80, 126.84, 125.43, 125.11, 124.32, 124.17, 124.03, 120.21, 120.15, 115.56, 108.00, 66.59, 48.50, 26.31.

HRMS (ESI MS) m/z: theor: 957.2543 found: 957.2541 ($M^{+\cdot}$ detected).

2.1.4. Synthesis of **Cu3**

A mixture of tetrakis(acetonitrile)copper(I) hexafluorophosphate (372 mg, 1.0 mmol, M = 372.72 g/mol) and *bis*[2-(diphenylphosphino)phenyl] ether (538 mg, 1.0 mmol, M = 538.57 g/mol) in 100 mL of dichloromethane was stirred at 25 °C for 2 h and then treated with a solution of 5,6-epoxy-5,6-dihydro-[1,10]phenanthroline (196 mg, 1.0 mmol, M = 196.20 g/mol) in 50 mL of dichloromethane. This reaction mixture was stirred for an additional 1 h and filtered and the clear yellow filtrate concentrated to 5 mL. Diethyl ether was added into the resulting solution afforded yellow crystals of the complex (878 mg, 93% yield).

^{1}H NMR (300 MHz, $CDCl_3$) δ 8.40 (d, J = 4.9 Hz, 2H), 8.21 (d, J = 7.5 Hz, 2H), 7.41 (dd, J = 7.7, 5.1 Hz, 2H), 7.35 – 7.12 (m, 14H), 7.11 – 6.85 (m, 12H), 6.83 – 6.67 (m, 2H), 4.77 (s, 2H).

^{13}C NMR (101 MHz, $CDCl_3$) δ 158.57, 149.39, 149.17, 147.79, 146.92, 139.78, 138.82, 134.57, 134.41, 133.25, 132.95, 132.11, 131.80, 130.36, 129.06, 128.97, 126.47, 126.23, 125.50, 125.12, 124.20, 120.90, 120.10, 54.78.

HRMS (ESI MS) m/z: theor: 797.1543 found: 797.1547 ($M^{+\cdot}$ detected).

2.1.5. Synthesis of **Cu4**

A mixture of tetrakis(acetonitrile)copper(I) hexafluorophosphate (372 mg, 1.0 mmol, M = 372.72 g/mol) and 4,5-*bis*(diphenylphosphino)-9,9-dimethylxanthene (578 mg, 1.0 mmol, M = 578.62 g/mol) in 100 mL of dichloromethane was stirred at 25 °C for 2 h and then treated with a solution of 5,6-epoxy-5,6-dihydro-[1,10]phenanthroline (196 mg, 1.0 mmol, M = 196.20 g/mol) in 50 mL of dichloromethane. This reaction mixture was stirred for an additional 1 h and filtered and the clear yellow filtrate concentrated to 5 mL. Diethyl ether was added into the resulting solution afforded yellow crystals of the complex. (895 mg, 91% yield)

^{1}H NMR (300 MHz, $CDCl_3$) δ 8.25 (d, J = 7.5 Hz, 2H), 8.08 (d, J = 4.8 Hz, 2H), 7.66 (ddd, J = 7.7, 4.8, 1.3 Hz, 2H), 7.41 (dd, J = 7.6, 5.1 Hz, 2H), 7.30 – 7.19 (m, 6H), 7.11 (dt, J = 15.4, 7.3 Hz, 8H), 6.97 – 6.87 (m, 4H), 6.83 (dd, J = 11.0, 6.8 Hz, 4H), 6.55 (dtd, J = 7.7, 6.3, 3.3 Hz, 2H), 4.81 (s, 2H), 1.77 (s, J = 8.3 Hz, 6H).

^{13}C NMR (101 MHz, $CDCl_3$) δ 154.99, 148.80, 147.31, 146.97, 140.10, 137.04, 136.03, 134.05, 132.97, 132.90, 132.81, 132.77, 132.68, 132.61, 132.32, 131.54, 131.34, 131.28, 131.18, 131.00, 130.81, 130.22, 130.19, 129.10, 129.04, 129.00, 128.94, 127.41, 127.36, 127.18, 126.44, 125.41, 125.29, 120.00, 119.84, 54.83, 36.30, 28.26.

HRMS (ESI MS) m/z: theor: 837.1856 found: 837.1859 ($M^{+\cdot}$ detected).

2.2. Light absorption properties of the investigated ligand and copper complexes

UV-Visible absorption spectra of all complexes and the ligand were determined in dichloromethane in order to select the most appropriate light source for photopolymerization experiments. Molar extinction coefficients of the ligand and the different copper complexes in dichloromethane (see Figure 1) and the light absorption characteristics are presented in Table 1 respectively. As shown in Figure 2, the maximum absorption wavelengths (λ_{max}) of **Cu1** and **Cu2** were all around 430 nm. Conversely, the light absorption properties of **Cu3** and **Cu4** differ from that of **Cu1** and **Cu2,** and their absorption maxima located at around 400 nm. These results clearly evidenced the influence of the ancillary ligand on the light absorption properties of the different Cu complexes. On the opposite, no influence on the absorption properties was detected for the phosphorylated ligand. Interestingly, the molar extinction coefficients of **Cu1**, **Cu2** were much higher than that of **Cu3**, **Cu4** at their maximum absorption wavelengths(λ_{max}) due to the ligand **A1** on **Cu1** and **Cu2** showed improved light absorption properties ($\varepsilon_{A\,1}$=97348 $M^{-1}\cdot cm^{-1}$ at λ_{max}=357 nm) (see Table 1). Thus, **Cu1** and **Cu3** exhibited molar extinction coefficients of $\varepsilon_{Cu\,1}$=26020 $M^{-1}\cdot cm^{-1}$ at λ_{max}=429 nm and $\varepsilon_{Cu\,3}$=15020 $M^{-1}\cdot cm^{-1}$ at λ_{max}=407 nm respectively.

Considering their absorption properties, all compounds were appropriate for photopolymerization experiments done at 405 nm so that their molar extinction coefficients at this wavelength were also determined (ε_{405nm}). Except for **A1**, molar extinction coefficients of other samples did not drop significantly at 405 nm. Compared to all, **Cu1** still showed the highest molar extinction coefficients at 405 nm (ε_{405nm}=23090 $M^{-1}\cdot cm^{-1}$), followed by **Cu2** (ε_{405nm}=21070 $M^{-1}\cdot cm^{-1}$). Logically, **Cu4** exhibited the lowest molar extinction coefficient at 405 nm, peaking at ε_{405nm}=9290 $M^{-1}\cdot cm^{-1}$.

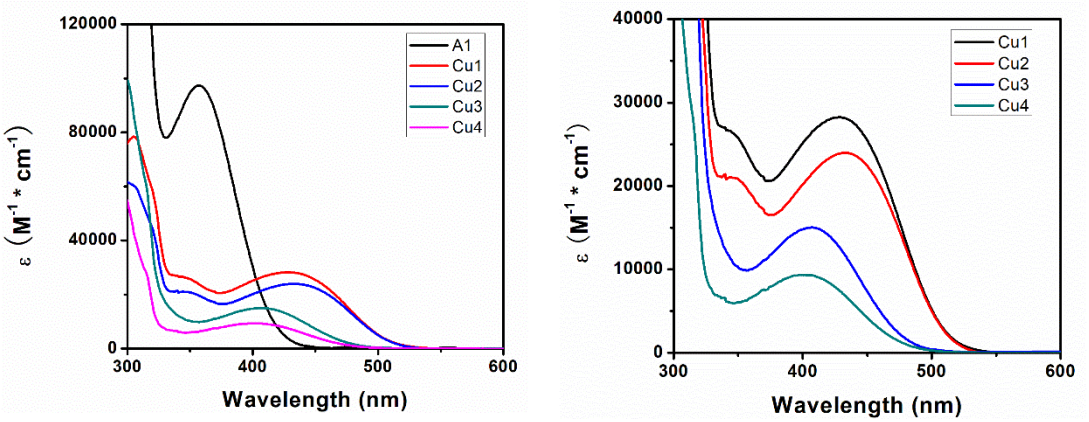

(**a**) (**b**)

Figure 1. UV-visible absorption spectra in dichloromethane of **(a) A1**, **Cu1**, **Cu2**, **Cu3** and **Cu4**; **(b) Cu1**, **Cu2**, **Cu3** and **Cu4**.

Table 1. Light absorption properties of the different complexes in dichloromethane: maximum absorption wavelengths λ_{max}; molar extinction coefficients at λ_{max} (ε_{max}) and extinction coefficients at the emission wavelength of the LED@405 nm(ε_{405nm}).

	λ_{max} (nm)	ε_{max}($M^{-1}\cdot cm^{-1}$)	ε_{405nm}($M^{-1}\cdot cm^{-1}$)
A1	357	97350	22440
Cu1	429	26030	23090
Cu2	433	23980	21070
Cu3	407	15020	15000
Cu4	398	9340	9290

2.3. Steady-state photolysis of the investigated ligand and copper complexes

In the typical three/two-component systems, the formation of free radicals is usually determined by the interaction between the complexes and the additives (Iod and/or amine). In order to study the interaction kinetics of compounds in the system upon light irradiation, steady-state photolysis experiments were carried out upon LED@405nm irradiation in dichloromethane. For **A1**, when irradiated without any additives, almost no photoreaction could be detected after 100 s of irradiation, which was reflected by the slight decrease of the UV-visible absorption peak at about 350 nm (see Figure 2a). The different situation was found during the photolysis of **Cu1**, **Cu2** (see Figure 3a and S2a respectively), **Cu3** and **Cu4** (see Figure 4a and S3a). It showed remarkable stability of investigated copper complexes upon irradiation. While examining the photolysis of the three-component **A1** (or **Cu1**, **Cu2**)/Iod/amine system, a completely different behavior was evidenced. Thus, for **A1**, the absorption peak at 360 nm underwent a significant decrease during light irradiation with the LED@405 nm, while two shoulder peaks at 325 nm and 440 nm appeared and increased (see Figure 2b). This was indicative of the formation of new photoproducts generated by interaction of **A1** with the different additives. A similar situation was found for **Cu1** and **Cu2** (see Figure 3b and S2b) and **A1**. In this case, appearance of only one absorption peak and one shoulder peak was detected. Interestingly, photolysis rates of **Cu3** and **Cu4** were very slow compared to the other three presented compounds (see Figure 4b and S3b), which support the much lower photoinitiation ability.

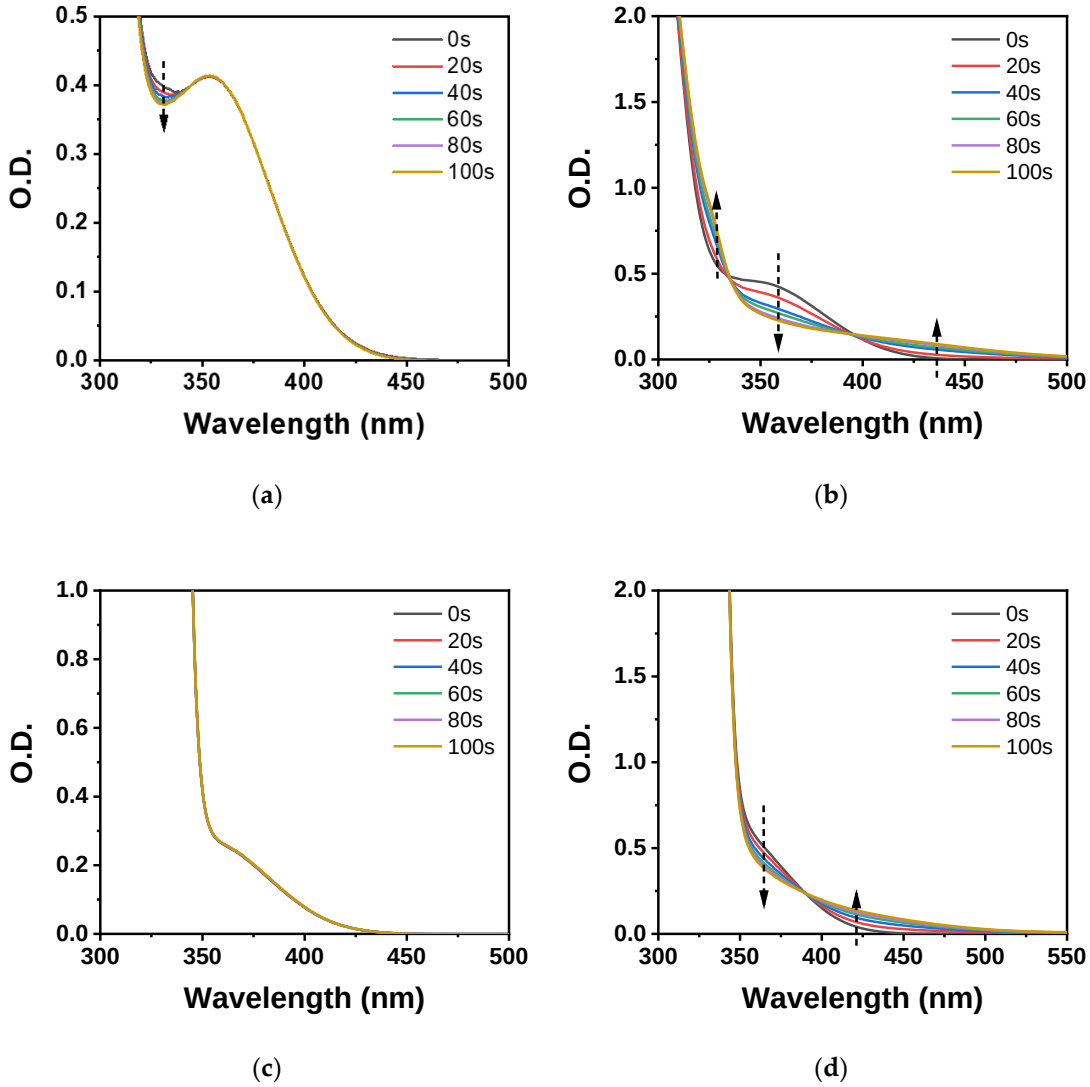

Figure 2. UV-visible absorption spectra of **A1** in dichloromethane: **(a)** without additives, **(b)** with both Iod and EDB, **(c)** with EDB and **(d)** with Iod upon exposure to LED@405nm under air for different times.

In the meantime, photolysis of all compounds/Iod or amine was performed for a more in-depth study of the interactions occurring in all photoinitiating systems. Thus, very slight changes were found in the UV-Visible absorptions of the two-component PISs for all compounds with amine (EDB) after light irradiation (see Figure 2c, 3c, 4c, S2c, S3c). It can thus be concluded that the chemical interaction between the different compounds and amine was very slow. In the meantime, the compounds/Iod systems demonstrated higher reactivity than that of the compounds/EDB systems during the photolysis experiments (see Figure 2d, 3d, 4d, S2d, S3d). The reaction curves of **Cu1** and **Cu2** were more similar to those of Iod owing to the similarity of the ligands present, with only minor differences in the reaction rates. The absorption peak at 430 nm decreased and then increased as the reaction proceeded, indicating that the reduction of the compounds in the reaction system was accompanied by the formation of new photoproducts. This was corroborated by the rising shoulder peak at 450 nm and beyond. This phenomenon was not detected for **Cu3** and **Cu4**, where only a decrease of the absorption peak located at 400 nm could be detected. At the same time, it was worth noting that the reaction rates of **Cu3** and **Cu4** with Iod were significantly slower compared to those of **Cu1** and **Cu2**(100 s vs. 300 s). This also coincided with the difference in the reaction rates of the photopolymerization profiles mentioned in the previous section.

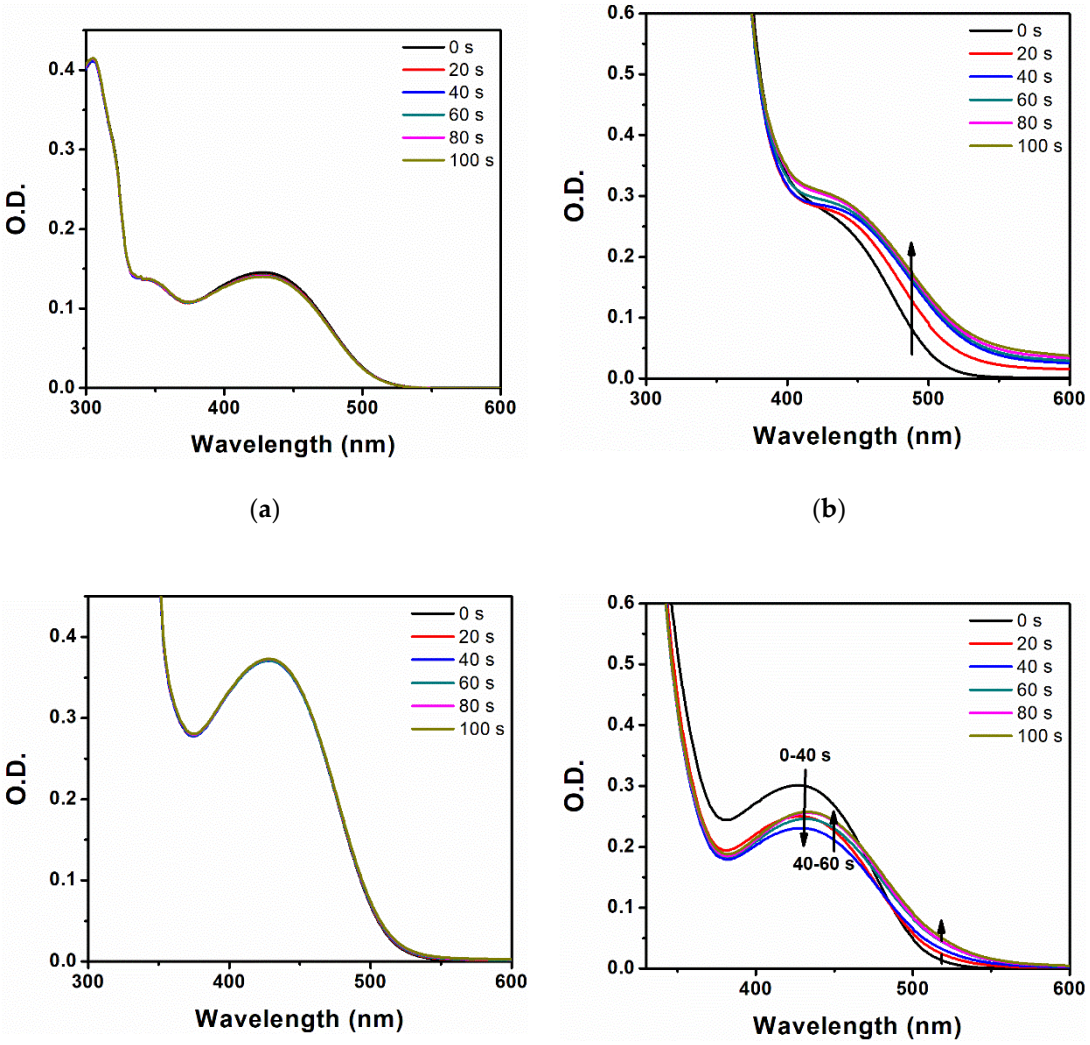

Figure 3. UV-visible absorption spectra of **Cu1** in dichloromethane: **(a)** without additives, **(b)** with both Iod and EDB, **(c)** with EDB and **(d)** with Iod upon exposure to LED@405nm under air for different times.

Although the consumption of the different compounds in the two-component system prepared with the amine were lower than that observed for those prepared with Iod, it can be concluded from the higher efficiency of the compounds/Iod interaction of a higher contribution of this system in photoinitiation compared to that provided by the compounds/EDB system. The new photoproducts were generated in the three-component systems of **Cu3** and **Cu4** instead of two-component systems. Besides, the oxidative and reductive interactions both contributed to the overall initiation generated by the three-component systems.

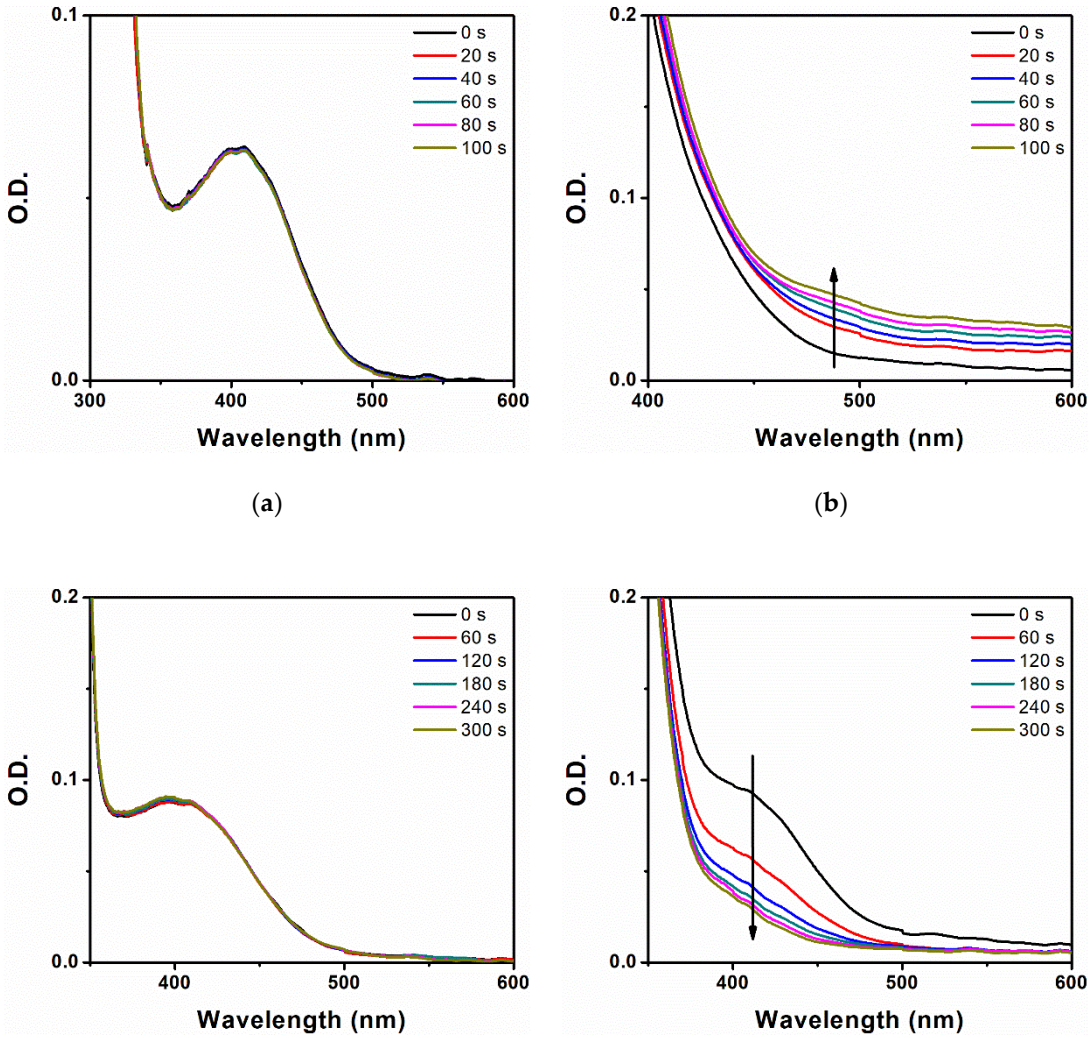

Figure 4. UV-visible absorption spectra of **Cu3** in dichloromethane: **(a)** without additives, **(b)** with both Iod and EDB, **(c)**with EDB and **(d)** with Iod upon exposure to LED@405nm under air for different times.

2.4. Chemical mechanisms in Photolysis Reactions

In previous reports,[12,45] the chemical mechanism generated by the copper complexes-based PISs were determined and presented in Scheme 2. Thus, upon irradiation, Cu(I) is promoted in the excited state (*Cu(I)), which can react with Iod and EDB in two different reactions r2 and r3, respectively. Through a series of redox reactions, new free radicals can be constantly produced.

$$Cu(I) \rightarrow {}^{*}Cu(I)\ (h\nu) \qquad (r1)$$

$${}^{*}Cu(I) + Ar_2I^{+} \rightarrow Cu(II) + Ar^{\bullet} + Ar\text{-}I \qquad (r2)$$

$$Cu(II) + EDB \rightarrow Cu(I) + EDB^{\bullet+} \qquad (r3)$$

Scheme 2. Proposed Mechanisms for the Copper Complexes/Iod/Amine Redox Combination.

2.5. ESR spin-trapping experiments for investigated ligand and copper complexes.

ESR spin trapping experiments were performed on **Cu1**/Iod and **Cu1**/EDB to further investigate the nature of the radicals generated from the reactions. As shown in Figures 5a and 5b, the phenyl radicals were detected for the **Cu1**/Iod PIS after 30 s irradiation with a LED@405 nm (a_N=14.3 G, a_H=2.3 G). It indirectly proved that r2 (see Scheme 2)

was occurring in the reaction medium. Additionally, the hyperfine coupling constants of a_N = 14.1 G and a_H = 2.1 G were indicative of the redox reaction (see Scheme 2, r3) occurring between **Cu1** and EDB (see Figure 5c and 5d). The aminoalkyl radical ($EDB_{(-H)}$•) arised from the reaction in which EDB was acting as a reductant. It is consistent with the relevant and previous reports.[47] Compared to **Cu1**/Iod PIS, the reaction rate of **Cu1**/EDB PIS was lower, which means that the radical adduct can be generated within a shorter time (30 s vs. 90 s) in **Cu1**/Iod PIS. It matches with the results of photolysis experiments.

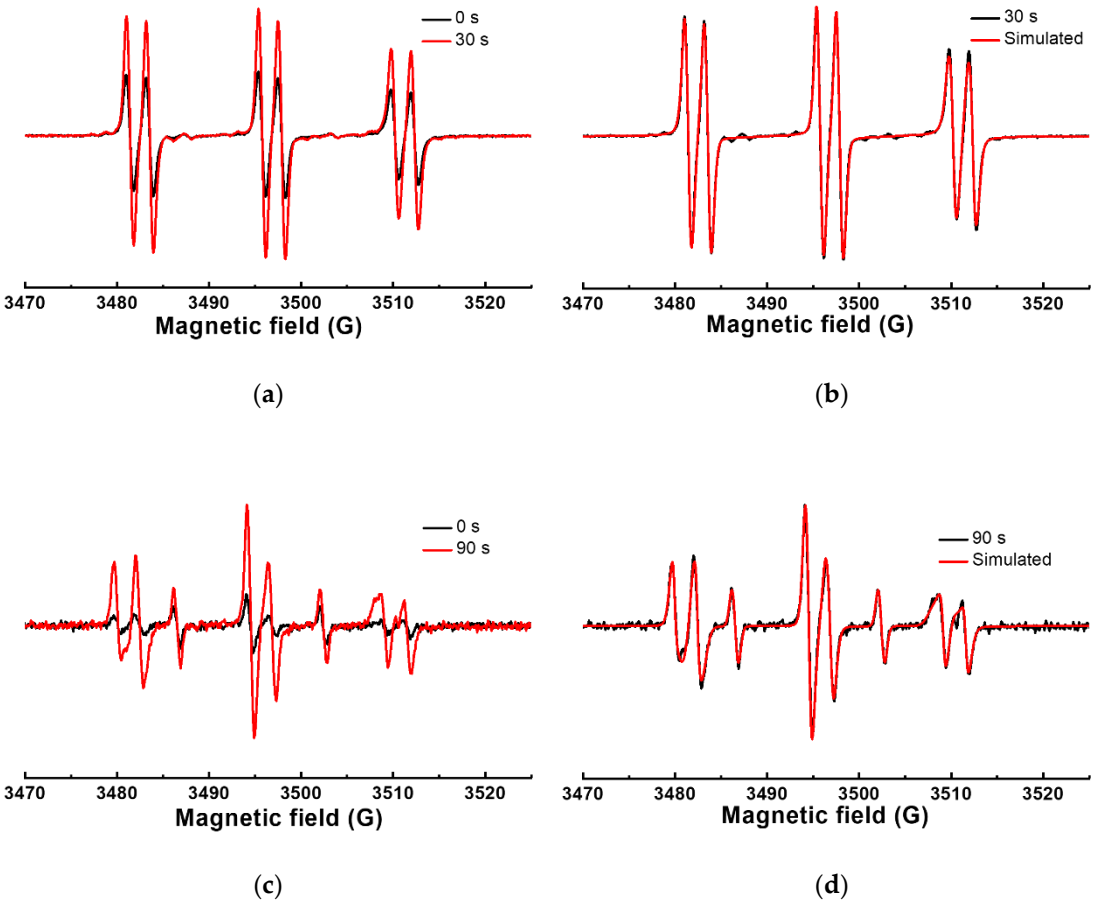

Figure 5. ESR spectra obtained from ESR-spin trapping experiments under irradiation with a LED emitting at 405 nm using PBN = 2 mg/mL (as the spin trap agent); Iod = 2 mg/mL, EDB = 2 mg/mL and **Cu1**= 0.2 mg/mL in *tert*-butylbenzene under N_2. (a) **Cu1**/Iod PIS, Irradiation time = 30 s (red) and = 0 s (black) spectra, respectively; (b) **Cu1**/Iod PIS, Irradiation time = 30 s experimental (black) and simulated (red) spectra; (c) **Cu1**/EDB PIS, Irradiation time = 90 s (red) and = 0 s (black) spectra; (d) **Cu1**/EDB PIS, Irradiation time = 90 s experimental (black) and simulated (red) spectra.

2.6. Photoinitiation ability of the investigated ligand and copper complexes.

Free radical polymerization profiles of TMPTA in laminate upon exposure with the LED at 405 nm by using real-time FTIR are shown in Figure 6. All the three-component photoinitiating systems were based on compounds:Iod:EDB = 0.2%:2%:2%, w/w/w. To evidence the efficiency of the three-component systems, a two-component PIS (Iod:EDB=2%:2%, w/w) was used as the blank system. Similarly, the cationic polymerization profiles of EPOX are also presented in Figure S1. Based on the previous study, and to clarify the results more clearly, the investigated compounds were divided into two different groups.

1. For **A1**, **Cu1** and **Cu2**, final acrylate function conversions around 50%~62% could be obtained in thin films (see Figure 1), which were higher than the conversions obtained with the reference two-component system. In this case, after less than 25 s of irradiation, higher monomer conversions could be determined for **Cu1** and **Cu2**, the corresponding systems being more reactive than the others. In EPOX, Cu1 showed an excellent photoinitiation ability that far exceeded that of the other compounds. The final epoxide function conversions achieved ~78% (see Figure S1). Considering that **Cu1** can efficiently initiate the polymerization of acrylates and epoxides, this complex was logically used as a photoinitiator for the elaboration of IPNs based on the polymerization of the blend of TMPTA and EPOX.

The initiation ability for the blank two-component system was ascribed to the formation to a photosensitive charge transfer complex between amine and iodonium salt.

2. For **Cu3** and **Cu4**, after overcoming the oxygen inhibition in thin films, highly efficient processes were noticed to have full polymerization within 100s. The final acrylate function conversions were around 80%, which was significantly higher than that obtained with the **A1**, **Cu1,** or **Cu2** based photoinitiating systems.

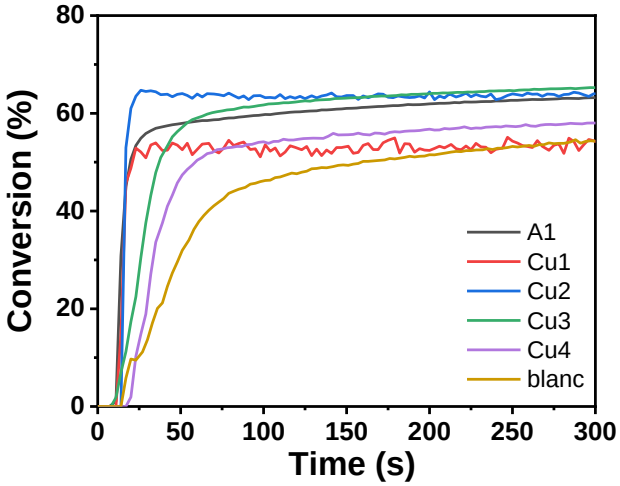

Figure 6. Photopolymerization profiles of TMPTA (acrylate function conversion vs irradiation time) initiated by compounds/Iod/EDB based three-component PISs (0.2%:2%:2%, w/w/w) upon irradiation to LED@405 nm in laminate in thin films, blank for Iod: EDB = 2%:2% (w/w). Irradiation starts at t = 10 s.

Overall, **A1**, **Cu1** and **Cu2** were highly efficient for the polymerization of TMPTA in thin films whereas **Cu1** could also efficiently initiate the photopolymerization of EPOX. Therefore, the photoinitiation abilities of **A1**, **Cu1** and **Cu2** perfectly fit with the chemical mechanisms and the light absorption properties mentioned above.

2.7. Direct laser writing (DLW) experiments

Considering the remarkable photoinitiation abilities of **A1**, **Cu1**, **Cu3**, and **Cu4** under various conditions, we selected these different compounds for composing the three-component systems used during the DLW experiments. According to the polymerization behaviours in TMPTA and EPOX, **A1** or **Cu1**/Iod/EDB (0.2%:2%:2%, w/w/w) in IPN, TMPTA: EPOX=50%:50%) and **Cu3** or **Cu4**/Iod/EDB (0.2%:2%:2%, w/w/w) in TMPTA were examined as formulations for practical applications. By numerical optical microscopy, the different tridimensional patterns presented smooth surfaces and excellent spatial resolutions. It means that an efficient FRP process occurred with all these systems, and stable letter patterns could be obtained with a very short writing time via DLW (see Figure 7).

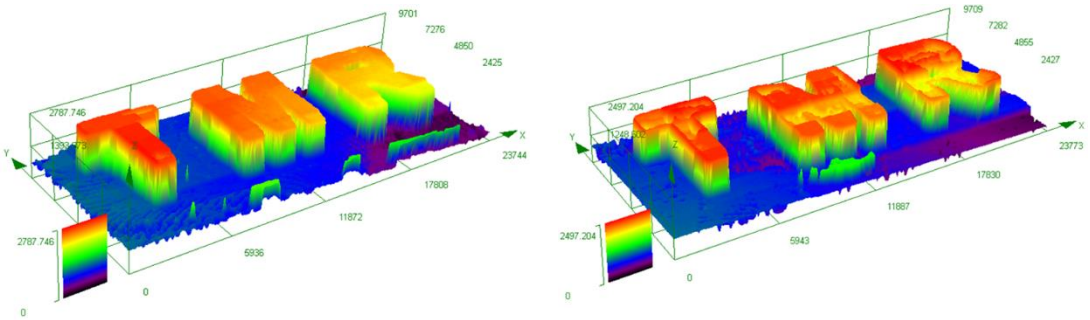

(**a**) (**b**)

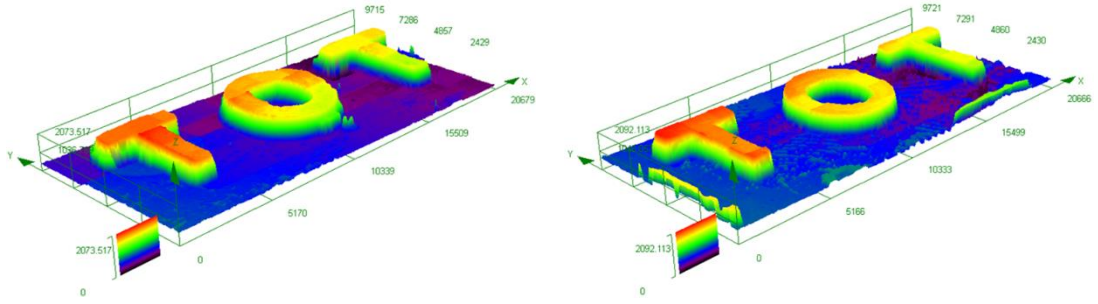

(**c**) (**d**)

Figure 7. Free radical photopolymerization experiments in DLW experiments. Characterization of 3D overall appearance of colour patterns determined by numerical optical microscopy in the presence of: (a) **A1**/Iod/EDB (0.2%/2%/2% in IPN, w/w/w); (b) **Cu1**/Iod/EDB (0.2%/2%/2% in IPN, w/w/w); (c) **Cu3**/Iod/EDB (0.2%/2%/2%/20% in TMPTA, w/w/w); (d) **Cu4**/Iod/EDB (0.2%/2%/2% in TMPTA, w/w/w).

3. Materials and Methods

3.1. Ligand and copper complexes

Chemical structures of the investigated ligand and the novel copper complexes are shown in Scheme 1. For the details of their synthetic procedures, please check Section 2.1.

3.2. Other materials used in the experiments

Chemical structures of the co-initiator i.e. the iodonium salt (Speedcure 938) and the electron donor i.e. the amine (ethyl dimethylaminobenzoate - EDB) are shown in Scheme 1. The reagents mentioned above were purchased from Lambson Ltd (UK). Trimethylolpropane triacrylate (TMPTA) and (3,4-epoxycyclohexane)methyl 3,4-epoxycyclohexylcarboxylate (EPOX) were obtained from Allnex and used as benchmark monomers for radical photopolymerization. Their chemical structures are presented in Scheme 1.

3.3. Polymerization profiles obtained by Real Time Fourier Transform Infrared Spectroscopy (RT-FTIR)

The novel copper complexes were dissolved with the iodonium salt (Iod) and the amine (EDB) in the benchmark monomers to prepare the photosensitive formulations. Their weight content ratios in monomer are: 0.2%/2%/2% w/w/w, respectively. The obtained formulations were deposited in laminate between two polypropylene films. Particularly, 1 or 2 drops are enough to control the thickness at ~ 100 µm, then the formulations were exposed to light by irradiating with a LED emitting at 405 nm (I0 = 110 mW.cm-2) to initiate the Free Radical Polymerization (FRP) at room temperature and under air. During the polymerization kinetics, the IR peak at ~ 6120 cm-1 and 3700 cm-1, corresponding to a characteristic peak of the TMPTA and EPOX, was continuously monitored by real-time FTIR spectroscopy (JASCO FTIR 4100). The polymerization profiles were established using the following relationship of acrylate function conversion at a given irradiation time:[7]

$$\text{conversion } (\%) = (A_0 - A_t)/A_0 \times 100 \quad (1)$$

where A_0 is the initial peak area before irradiation and A_t is the peak area after irradiation for a given time t.

3.4. The chemical mechanisms studies

To investigate the chemical mechanisms induced by the three-component PISs during photopolymerization, photolysis experiments measurements were carried out by UV-visible absorption spectroscopy (JASCO V730 UV–visible spectrometer) respectively.

3.5. Electron spin resonance spin trapping experiments

Electron spin resonance spin trapping (ESR-ST) experiments were performed by X-band spectrometry (Bruker EMXplus), and upon irradiation with a light source (LED@405 nm). For the capture of the generated free radicals, a *N*-*tert*-butyl-α-phenylnitrone (PBN) solution with certain concentration (in nitrogen-saturated *tert*-butylbenzene) were formulated at room temperature. Lastly, the simulations of ESR spectra were carried out with the help of PEST WINSIM software.[15,34]

3.6. 3D printing experiments

These experiments were carried out in a 2 mm thick homemade tank. Upon irradiation with a computer-controlled laser diode@405nm with spot size around 50 μm, tridimensional patterns were fabricated. Their precise shapes were characterized by a numerical optical microscope (DSX-HRSU, OLYMPUS corporation) after direct laser writing.[45]

4. Conclusions

In this article, a ligand A1 and four novel copper complexes with excellent photocatalytic abilities were designed and synthesized to efficiently promote photopolymerizations. Interestingly, **A1**, **Cu1**, **Cu2** and **Cu3**, **Cu4** can be divided into two groups based on the differences of structures. Besides, all compounds showed excellent photoinitiation abilities (short induction time or high final conversion) in different monomers and in thin films at 405 nm, respectively. The reactivity of the different compounds during photoreaction was studied by UV-Visible absorption spectroscopy. ESR spin trapping experiments were also successfully performed to characterize the photochemical mechanisms involved in the FRP of TMPTA. Finally, in order to realize the application of photopolymerization reaction in practical production life, DLW experiments with photoinitiating systems were performed to prepare the 3D patterns successfully.

Supplementary Materials: The following are available online at www.mdpi.com/xxx/s1, Figure S1: Photopolymerization profiles of EPOX; Figure S2: UV-visible absorption spectra of **Cu2**; Figure S3: UV-visible absorption spectra of **Cu4**.

Author Contributions: Conceptualization, J.L., F.D. and P.X.; synthesis of ligand and copper complexes, G.N., D.G. and F.D.; validation, all authors; formal analysis, J.L., F.D., P.X. and T.B.; data curation, all authors; writing—original draft preparation, J.L., F.D., P.X. and T.B.; writing—review and editing, all authors. All authors have read and agreed to the published version of the manuscript.

Funding: China Scholarship Council (CSC) for Timur Borjigin.

Acknowledgments: The authors wish to thank the Region Grand Est (France) for the grant "MIPPI-4D". This research project is supported by China Scholarship Council (CSC) (No.202007030005). PX acknowledges funding from the "Australian Research Council (FT170100301)".

Conflicts of Interest: The authors declare no conflict of interest.

References

1. Nicewicz, D.A.; MacMillan, D.W. Merging photoredox catalysis with organocatalysis: the direct asymmetric alkylation of aldehydes. *Science* **2008**, *322*, 77-80, doi:10.1126/science.1161976.
2. Renaud, P.; Leong, P. A light touch catalyzes asymmetric carbon-carbon bond formation. *ChemInform* **2009**, *40*, i, doi:10.1002/chin.200908263.
3. Nagib, D.A.; Scott, M.E.; MacMillan, D.W. Enantioselective α-trifluoromethylation of aldehydes via photoredox organocatalysis. *J. Am. Chem. Soc.* **2009**, *131*, 10875-10877, doi:10.1021/ja9053338.
4. Zeitler, K. Photoredox catalysis with visible light. *Angew. Chem. Int. Ed. Engl.* **2009**, *48*, 9785-9789, doi:10.1002/anie.200904056.
5. Shih, H.-W.; Vander Wal, M.N.; Grange, R.L.; MacMillan, D.W. Enantioselective α-benzylation of aldehydes via photoredox organocatalysis. *J. Am. Chem. Soc.* **2010**, *132*, 13600-13603, doi:10.1021/ja106593m.
6. Pham, P.V.; Nagib, D.A.; MacMillan, D.W. Photoredox Catalysis: A Mild, Operationally Simple Approach to the Synthesis of α - Trifluoromethyl Carbonyl Compounds. *Angew. Chem. Int. Ed.* **2011**, *50*, 6119-6122, doi:10.1002/anie.201101861.

7. Dietlin, C.; Schweizer, S.; Xiao, P.; Zhang, J.; Morlet-Savary, F.; Graff, B.; Fouassier, J.-P.; Lalevée, J. Photopolymerization upon LEDs: new photoinitiating systems and strategies. *Polym. Chem.* **2015**, *6*, 3895-3912, doi:10.1039/c5py00258c.
8. Allegrezza, M.L.; DeMartini, Z.M.; Kloster, A.J.; Digby, Z.A.; Konkolewicz, D. Visible and sunlight driven RAFT photopolymerization accelerated by amines: kinetics and mechanism. *Polym. Chem.* **2016**, *7*, 6626-6636, doi:10.1039/c6py01433j.
9. Wang, J.; Rivero, M.; Muñoz Bonilla, A.; Sanchez-Marcos, J.; Xue, W.; Chen, G.; Zhang, W.; Zhu, X. Natural RAFT Polymerization: Recyclable-Catalyst-Aided, Opened-to-Air, and Sunlight-Photolyzed RAFT Polymerizations. *ACS Macro. Lett.* **2016**, *5*, 1278-1282, doi:10.1021/acsmacrolett.6b00818.
10. Decker, C.; Bendaikha, T. Interpenetrating polymer networks. II. Sunlight ‐ induced polymerization of multifunctional acrylates. *J. Appl. Polym. Sci.* **1998**, *70*, 2269-2282, doi:10.1002/(SICI)1097-4628(19981212)70:11<2269::AID-APP21>3.0.CO;2-D.
11. Ciftci, M.; Tasdelen, M.A.; Yagci, Y. Sunlight induced atom transfer radical polymerization by using dimanganese decacarbonyl. *Polym. Chem.* **2014**, *5*, 600-606, doi:10.1039/C3PY01009K.
12. Xiao, P.; Zhang, J.; Campolo, D.; Dumur, F.; Gigmes, D.; Fouassier, J.P.; Lalevée, J. Copper and iron complexes as visible ‐ light ‐ sensitive photoinitiators of polymerization. *J. Polym. Sci., Part A: Polym. Chem.* **2015**, *53*, 2673-2684, doi:10.1002/pola.27762.
13. Allen, N.S. Photoinitiators for UV and visible curing of coatings: mechanisms and properties. *J. Photochem. Photobiol., A* **1996**, *100*, 101-107, doi:10.1016/S1010-6030(96)04426-7.
14. Grotzinger, C.; Burget, D.; Jacques, P.; Fouassier, J. Visible light induced photopolymerization: speeding up the rate of polymerization by using co-initiators in dye/amine photoinitiating systems. *Polymer* **2003**, *44*, 3671-3677, doi:10.1016/S0032-3861(03)00286-6.
15. Lalevée, J.; Blanchard, N.; Tehfe, M.-A.; Peter, M.; Morlet-Savary, F.; Gigmes, D.; Fouassier, J.P. Efficient dual radical/cationic photoinitiator under visible light: a new concept. *Polym. Chem.* **2011**, *2*, 1986-1991.
16. Zuo, X.; Morlet ‐ Savary, F.; Graff, B.; Blanchard, N.; Goddard, J.P.; Lalevée, J. Fluorescent Brighteners as Visible LED ‐ Light Sensitive Photoinitiators for Free Radical Photopolymerizations. *Macromol. Rapid Commun.* **2016**, *37*, 840-844, doi:10.1002/marc.201600103.
17. Tokura, Y.; Nagaosa, N. Orbital physics in transition-metal oxides. *Science* **2000**, *288*, 462-468, doi:10.1126/science.288.5465.462.
18. Hay, P.J. Gaussian basis sets for molecular calculations. The representation of 3 d orbitals in transition ‐ metal atoms. *J. Chem. Phys.* **1977**, *66*, 4377-4384, doi:10.1063/1.433731.
19. Marynick, D.S. . pi.-Accepting abilities of phosphines in transition-metal complexes. *J. Am. Chem. Soc.* **1984**, *106*, 4064-4065, doi:10.1021/ja00326a048.
20. Orgel, L. Spectra of transition ‐ metal complexes. *J. Chem. Phys.* **1955**, *23*, 1004-1014, doi:10.1063/1.1742182.
21. Lee, Y.; Yuan, S.; Sanchez, A.; Yu, L. Charge transport mediated by d-orbitals in transition metal complexes. *Chemical communications (Cambridge, England)* **2008**, 247-249, doi:10.1039/b712978e.
22. Prier, C.K.; Rankic, D.A.; MacMillan, D.W. Visible light photoredox catalysis with transition metal complexes: applications in organic synthesis. *Chem. Rev.* **2013**, *113*, 5322-5363, doi:10.1021/cr300503r.
23. Parasram, M.; Gevorgyan, V. Visible light-induced transition metal-catalyzed transformations: beyond conventional photosensitizers. *Chem. Soc. Rev.* **2017**, *46*, 6227-6240, doi:10.1039/c7cs00226b.
24. Zhao, J.; Ji, S.; Wu, W.; Wu, W.; Guo, H.; Sun, J.; Sun, H.; Liu, Y.; Li, Q.; Huang, L. Transition metal complexes with strong absorption of visible light and long-lived triplet excited states: from molecular design to applications. *RSC Adv.* **2012**, *2*, 1712-1728, doi:10.1039/C1RA00665G.
25. Huo, H.; Shen, X.; Wang, C.; Zhang, L.; Rose, P.; Chen, L.A.; Harms, K.; Marsch, M.; Hilt, G.; Meggers, E. Asymmetric photoredox transition-metal catalysis activated by visible light. *Nature* **2014**, *515*, 100-103, doi:10.1038/nature13892.

26. Kancherla, R.; Muralirajan, K.; Sagadevan, A.; Rueping, M. Visible light-induced excited-state transition-metal catalysis. *Trends in Chemistry* **2019**, *1*, 510-523, doi:10.1016/j.trechm.2019.03.012.
27. Fogel, Y.; Kastler, M.; Wang, Z.; Andrienko, D.; Bodwell, G.J.; Müllen, K. Electron-deficient N-heteroaromatic linkers for the elaboration of large, soluble polycyclic aromatic hydrocarbons and their use in the synthesis of some very large transition metal complexes. *J. Am. Chem. Soc.* **2007**, *129*, 11743-11749, doi:10.1021/ja072521t.
28. Seiders, T.J.; Baldridge, K.K.; O'Connor, J.M.; Siegel, J.S. Hexahapto metal coordination to curved polyaromatic hydrocarbon surfaces: The first transition metal corannulene complex. *J. Am. Chem. Soc.* **1997**, *119*, 4781-4782, doi:10.1021/ja964380t.
29. Maurer, A.B.; Meyer, G.J. Stark spectroscopic evidence that a spin change accompanies light absorption in transition metal polypyridyl complexes. *J. Am. Chem. Soc.* **2020**, *142*, 6847-6851, doi:10.1021/jacs.9b13602.
30. Choy, W.C.; Chan, W.K.; Yuan, Y. Recent advances in transition metal complexes and light‐management engineering in organic optoelectronic devices. *Adv. Mater.* **2014**, *26*, 5368-5399, doi:10.1002/adma.201306133.
31. Dighe, S.U.; Juliá, F.; Luridiana, A.; Douglas, J.J.; Leonori, D. A photochemical dehydrogenative strategy for aniline synthesis. *Nature* **2020**, *584*, 75-81, doi:10.1038/s41586-020-2539-7.
32. Wang, J.-S.; Matyjaszewski, K. Controlled/" living" radical polymerization. atom transfer radical polymerization in the presence of transition-metal complexes. *J. Am. Chem. Soc.* **1995**, *117*, 5614-5615, doi:10.1021/ja00125a035.
33. di Lena, F.; Matyjaszewski, K. Transition metal catalysts for controlled radical polymerization. *Prog. Polym. Sci.* **2010**, *35*, 959-1021, doi:10.1016/j.progpolymsci.2010.05.001.
34. Lalevée, J.; Blanchard, N.; Tehfe, M.-A.; Morlet-Savary, F.; Fouassier, J.P. Green bulb light source induced epoxy cationic polymerization under air using tris (2, 2′-bipyridine) ruthenium (II) and silyl radicals. *Macromolecules* **2010**, *43*, 10191-10195, doi:10.1021/ma1023318.
35. Lalevée, J.; Blanchard, N.; Tehfe, M.A.; Peter, M.; Morlet‐Savary, F.; Fouassier, J.P. A novel photopolymerization initiating system based on an iridium complex photocatalyst. *Macromol. Rapid Commun.* **2011**, *32*, 917-920, doi:10.1002/marc.201100098.
36. Lalevée, J.; Tehfe, M.-A.; Dumur, F.; Gigmes, D.; Blanchard, N.; Morlet-Savary, F.; Fouassier, J.P. Iridium photocatalysts in free radical photopolymerization under visible lights. *ACS Macro. Lett.* **2012**, *1*, 286-290, doi:10.1021/mz2001753.
37. Lalevée, J.; Peter, M.; Dumur, F.; Gigmes, D.; Blanchard, N.; Tehfe, M.A.; Morlet‐Savary, F.; Fouassier, J.P. Subtle ligand effects in oxidative photocatalysis with iridium complexes: application to photopolymerization. *Chem. Eur. J.* **2011**, *17*, 15027-15031, doi:10.1002/chem.201101445.
38. Tehfe, M.-A.; Gigmes, D.; Dumur, F.; Bertin, D.; Morlet-Savary, F.; Graff, B.; Lalevée, J.; Fouassier, J.-P. Cationic photosensitive formulations based on silyl radical chemistry for green and red diode laser exposure. *Polym. Chem.* **2012**, *3*, 1899-1902, doi:10.1039/C1PY00460C.
39. Lalevée, J.; Dumur, F.d.r.; Mayer, C.d.R.; Gigmes, D.; Nasr, G.; Tehfe, M.-A.; Telitel, S.; Morlet-Savary, F.; Graff, B.; Fouassier, J.P. Photopolymerization of N-vinylcarbazole using visible-light harvesting iridium complexes as photoinitiators. *Macromolecules* **2012**, *45*, 4134-4141, doi:10.1021/ma3005229.
40. Tehfe, M.-A.; Lalevée, J.; Telitel, S.; Sun, J.; Zhao, J.; Graff, B.; Morlet-Savary, F.; Fouassier, J.-P. Iridium complexes incorporating coumarin moiety as catalyst photoinitiators: Towards household green LED bulb and halogen lamp irradiation. *Polymer* **2012**, *53*, 2803-2808, doi:10.1016/j.polymer.2012.05.009.
41. Mokbel, H.; Anderson, D.; Plenderleith, R.; Dietlin, C.; Morlet-Savary, F.; Dumur, F.; Gigmes, D.; Fouassier, J.; Lalevee, J. Simultaneous initiation of radical and cationic polymerization reactions using the “G1” copper complex as photoredox catalyst: Applications of free radical/cationic hybrid photopolymerization in the composites and 3D printing fields. *Prog. Org. Coat.* **2019**, *132*, 50-61, doi:10.1016/j.porgcoat.2019.02.044.

42. Tehfe, M.A.; Lalevée, J.; Gigmes, D.; Fouassier, J.P. Combination of transition metal carbonyls and silanes: New photoinitiating systems. *J. Polym. Sci., Part A: Polym. Chem.* **2010**, *48*, 1830-1837, doi:10.1002/pola.23956.
43. Tar, H.; Kashar, T.I.; Kouki, N.; Aldawas, R.; Graff, B.; Lalevee, J. Novel Copper Photoredox Catalysts for Polymerization: An In Situ Synthesis of Metal Nanoparticles. *Polymers (Basel)* **2020**, *12*, 2293, doi:10.3390/polym12102293.
44. Al Mousawi, A.; Kermagoret, A.; Versace, D.-L.; Toufaily, J.; Hamieh, T.; Graff, B.; Dumur, F.; Gigmes, D.; Fouassier, J.P.; Lalevée, J. Copper photoredox catalysts for polymerization upon near UV or visible light: Structure/reactivity/efficiency relationships and use in LED projector 3D printing resins. *Polym. Chem.* **2017**, *8*, 568-580, doi:10.1039/C6PY01958G.
45. Xiao, P.; Dumur, F.; Zhang, J.; Fouassier, J.P.; Gigmes, D.; Lalevée, J. Copper complexes in radical photoinitiating systems: applications to free radical and cationic polymerization upon visible LEDs. *Macromolecules* **2014**, *47*, 3837-3844, doi:10.1021/ma5006793.
46. Garra, P.; Dumur, F.; Gigmes, D.; Al Mousawi, A.; Morlet-Savary, F.; Dietlin, C.; Fouassier, J.; Lalevée, J. Copper (photo) redox catalyst for radical photopolymerization in shadowed areas and access to thick and filled samples. *Macromolecules* **2017**, *50*, 3761-3771, doi:10.1021/acs.macromol.7b00622.
47. Tomal, W.; Pilch, M.; Chachaj-Brekiesz, A.; Galek, M.; Morlet-Savary, F.; Graff, B.; Dietlin, C.; Lalevée, J.; Ortyl, J. Photoinitiator-catalyst systems based on meta-terphenyl derivatives as photosensitisers of iodonium and thianthrenium salts for visible photopolymerization in 3D printing processes. *Polym. Chem.* **2020**, *11*, 4604-4621, doi:10.1039/D0PY00597E.